

# Experimental Validation of Relative Attitude Determination through Line of Sight Measurements for a Two-Vehicle Static Formation

Fatak Borhani and Niranjana Ravichandra  
 University at Buffalo, State University of New York  
 Department of Mechanical & Aerospace Engineering  
 Amherst, NY 14260-4400  
 fatakbor@buffalo.edu, nraivicha@buffalo.edu

**Faculty Advisor:** John L. Crassidis  
 University at Buffalo, State University of New York

## ABSTRACT

Experimental results for testing the validity of GPS-denied relative attitude determination for a two-vehicle formation using line-of-sight (LOS) measurements in a static setting are presented. The experiments are conducted in the VICON environment. The estimated relative attitude given by the system is compared to the true relative attitude, computed using the LOS solution. The attitude covariance matrix is compared to the relative attitude angle errors to demonstrate performance characteristics.

## INTRODUCTION

Formation flight enables multiple vehicles to collaborate in a single mission, improving mission success through cooperative achievement of the team's goal. Examples of applications in air, sea, and space include formation flight for enhanced aerodynamic efficiency [7], surveillance and reconnaissance using autonomous underwater vehicles, and satellite formation flying for coverage control [9]. However, flying in formation also requires each vehicle to maintain a specific orientation (attitude) with respect to other vehicles in the formation, which is known as relative attitude. Many of the current methods for formation flying rely on the use of the Global Positioning System (GPS) to determine vehicle attitude. However, GPS is not always available and is vulnerable to jamming in an adversarial setting. Therefore, it is important to create and implement algorithms that can extract relative attitude information without relying on GPS or other GPS-like methods.

There are existing Vision-based Navigation (VISNAV) methods for determining the vehicle attitude in GPS-denied environments, however such methods require significant computational power, onboard. A better alternative may be the incorporation of laser communication devices on each vehicle for determination of line-of-sight

(LOS) vectors between pairwise vehicles and jointly observed objects in the environment to compute the relative attitude. Laser-ranging hardware requires significantly less computational power and is not dependent on a global positioning service. These devices are also far less expensive to purchase and implement and, therefore, are considered to be more viable, economically.

In Ref. [1], a new algorithm is introduced to compute the full relative attitude of two vehicles in formation using the LOS vectors. The algorithm incorporates LOS vectors between the two vehicles and a commonly observed object with unknown position information to achieve a deterministic solution. This paper experimentally validates the aforementioned algorithm using the VICON motion capture system, with the objective of determining the accuracy of the solution presented in Ref. [1]. The results are validated by comparing the experimentally obtained characteristics of a two-vehicle system, including the attitude, with the characteristics derived from the LOS solution.

The organization of this paper is as follows. First, a discussion on the nature of the problem is given. This is followed by a brief summary of the specific constrained solution used during the validation process. Then, the experimental setup, data acquisition and processing methods are discussed, including a discussion on the errors using a

number of statistical tests. We conclude with the comparison between attitude covariance matrices and the relative attitude angle errors to demonstrate the reliability and accuracy of the algorithm.

## PROBLEM DEFINITION

With Figure 1 as reference, we consider the case where two vehicles are flying in formation. Each has a separate body frame denoted  $\mathcal{B}_1$  and  $\mathcal{B}_2$ , respectively. In this case, the relative attitude matrix mapping the relative orientation between frames  $\mathcal{B}_1$  and  $\mathcal{B}_2$  can be represented as  $A_{\mathcal{B}_1}^{\mathcal{B}_2} = A_{\mathcal{B}_2}^{\mathcal{I}^T} A_{\mathcal{B}_1}^{\mathcal{I}}$ , where  $\mathcal{I}$  denotes the inertial frame [1].

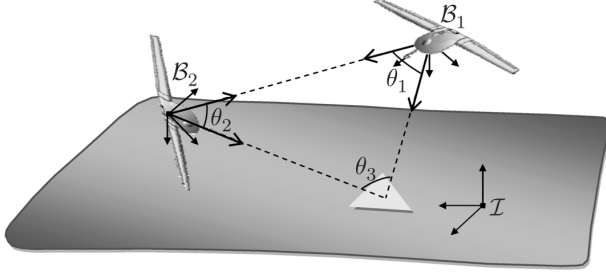


**Figure 1: Vehicle Formation**

Each vehicle observes a LOS from itself to both another in the formation as well as a common reference object such as a landmark. All four LOS vectors required to compute the full relative attitude of each vehicle in the system can be defined as follows:

- Vector  $\mathbf{v}_1$  is the LOS from  $\mathcal{B}_2$  to  $\mathcal{B}_1$ , expressed in  $\mathcal{B}_1$  coordinates.
- Vector  $\mathbf{w}_1$  is the LOS from  $\mathcal{B}_2$  to  $\mathcal{B}_1$ , expressed in  $\mathcal{B}_2$  coordinates.
- Vector  $\mathbf{v}_2$  is the LOS from  $\mathcal{B}_1$  to the common object, expressed in  $\mathcal{B}_1$  coordinates.
- Vector  $\mathbf{w}_2$  is the LOS from  $\mathcal{B}_2$  to the common object, expressed in  $\mathcal{B}_2$  coordinates.

Figure 2 details the discussed two-vehicle formation geometry with  $\mathcal{B}_1$  and  $\mathcal{B}_2$  as the vehicles of interest and the common-observed object as the third object in the formation. The LOS observations and directions of the unit vectors are also laid out [1].

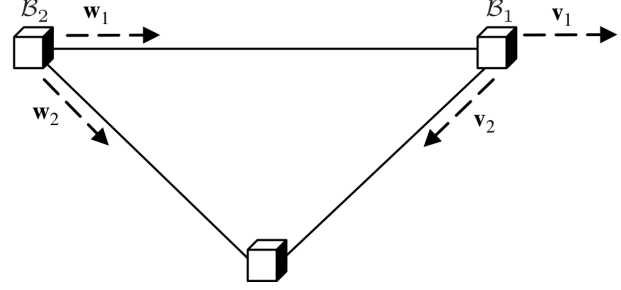


**Figure 2: Observation geometry**

The vectors  $\mathbf{v}_1$  and  $\mathbf{w}_1$  are required to be aligned based on the observation geometry. Since they are described in two different body coordinate systems the two vectors can be related through the mapping equation

$$\mathbf{w}_1 = A_{\mathcal{B}_1}^{\mathcal{B}_2} \mathbf{v}_1 \quad (1)$$

It is clear that only these two LOS vectors are not sufficient to compute the full relative attitude of the two vehicles as they do not provide an input on the rotation angle about the observation vector. So to determine the full three-axis relative attitude of the vehicles, this rotation angle must also be known. This is shown by

$$d = \mathbf{w}_2^T A_{\mathcal{B}_1}^{\mathcal{B}_2} \mathbf{v}_2 \quad (2)$$

where  $d$  is the cosine of the angle between the two LOS vectors to the common object. Also, we denote  $A_{\mathcal{B}_1}^{\mathcal{B}_2}$  as simply  $A$  from here on, for ease of reference. For the equations to be used directly, the angle between  $\mathbf{w}_2$  and  $\mathbf{v}_2$  must be observed by the third object in the formation. However, since they constitute the legs of a triangle (in accordance with Figure 1) and the angles in a triangle must add up to  $\pi$ , the angles are dependent on one another. Hence, if two of the angles are known, then the third can be determined. Since for the observation geometry considered, all LOS vectors lie on a common plane, a plane constraint can also be used to solve for the rotation angle. Then the LOS vectors between two frames can be aligned, after which a rotation angle about the reference direction can be found such that when the rotation is applied, the angle between the observations add up to  $\pi$  or the vectors lie on the same plane. Hence, the third reference object does not need to communicate its LOS observations to the two vehicles to determine their relative attitude [1].

Therefore, the choice of the common-observed object is completely arbitrary, and can be any common reference point with unknown position when the geometrical condition is applied. This is a strong conclusion and widely increases the desirability of the algorithm, especially in adversarial situations or search and rescue operations where the mission success must be achieved with minimal infor-

mation about the environment [1]. The condition is applied in the form of a constraint. Two are considered, one where the observation vectors are constrained by lying on the same plane—the planar constraint—and the other when the angles between the LOS vectors are constrained to add up to  $\pi$ —the triangle constraint.

The planar constraint can be described as

$$0 = \mathbf{w}_2^T [\mathbf{w}_1 \times] \mathbf{A} \mathbf{v}_2 \quad (3)$$

where the matrix  $[\mathbf{w}_1 \times]$  is the cross product matrix. The definition of cross product matrix for a general  $3 \times 1$  vector  $\alpha$  is [2]

$$[\alpha \times] \equiv \begin{bmatrix} 0 & -\alpha_3 & \alpha_2 \\ \alpha_3 & 0 & -\alpha_1 \\ -\alpha_2 & \alpha_1 & 0 \end{bmatrix} \quad (4)$$

The planar constraint is a less rigorous constraint compared to the triangle constraint, as there are two possible configurations that satisfy it. The first configuration is the actual observation geometry and the second is the case where  $\mathbf{A} \mathbf{v}_2$  vector is rotated by  $\pi$  rad from the true configuration, hence, a twofold ambiguity in the final solution.

A more rigorous constraint is where the angles between the vectors are constrained. The constraint function is defined as

$$\theta_3 = \pi - \theta_1 - \theta_2 \quad (5)$$

where the angles are defined in Figure 1. After taking cosines of both sides of Eq. (5), the dot product and cross product are used to obtain the cosine and sine of the angles in terms of the observations. Then, the final form of the triangle constraint is given by

$$\mathbf{w}_2^T \mathbf{A} \mathbf{v}_2 = \mathbf{w}_2^T \mathbf{w}_1 \mathbf{v}_1^T \mathbf{v}_2 + \|\mathbf{w}_1 \times \mathbf{w}_2\| \|\mathbf{v}_1 \times \mathbf{v}_2\| \quad (6)$$

Using Eq. (2) to replace the left hand side of Eq. (6), the angle observation equation in Eq. (6) becomes [1]

$$d = \mathbf{w}_2^T \mathbf{w}_1 \mathbf{v}_1^T \mathbf{v}_2 + \|\mathbf{w}_1 \times \mathbf{w}_2\| \|\mathbf{v}_1 \times \mathbf{v}_2\| \quad (7)$$

## CONSTRAINED SOLUTION

In order to effectively determine an attitude matrix that describes the mapping between  $\mathcal{B}_1$  and  $\mathcal{B}_2$  the conditions laid out in Eq. (1) and Eq. (7) must be satisfied. First, a rotation matrix describing the mapping of vectors  $\mathbf{v}_1$  and  $\mathbf{w}_1$  must be determined. This is achieved using a general rotation  $B = R(\mathbf{n}_1, \theta)$  about an arbitrary axis  $\mathbf{n}_1$ , by some angle  $\theta$ . For this purpose, the vector between the two vehicles has been selected in Ref. [1] and, thus, the initial

rotation can be described as the following, in which case  $\theta$  is  $\pi$  rad:

$$B = \frac{(\mathbf{w}_1 + \mathbf{v}_1)(\mathbf{w}_1 + \mathbf{v}_1)^T}{1 + \mathbf{v}_1^T \mathbf{w}_1} - I_{3 \times 3} \quad (8)$$

The rotation ensures that the LOS observations between the vehicles are aligned with each other. However, it is not guaranteed that the frames do not have a rotation about this LOS vector. Therefore, to compute the final rotation matrix  $A$ , a secondary rotation about this vector by some rotation angle must take place, and hence that rotation angle must be determined. Eventually, the full relative attitude can be written as

$$A = R(\mathbf{n}_2, \theta) B \quad (9)$$

The following is a summary of how the rotation angle is obtained, as detailed in Ref. [1]. Due to the ambiguity of the planar constraint, the final rotation angle is determined using the triangle constraint, which provides a unique solution by constraining the sum of the internal angles to  $\pi$  rad.

## Triangle Constraint

Since Eq. (1) is now satisfied, the above equation can be used as an input to Eq. (7) and the required rotation angle  $\theta$  can be determined. This substitution results in the following:

$$d = \mathbf{w}_2^T R(\mathbf{n}_2, \theta) \mathbf{w}^* \quad (10)$$

where  $\mathbf{w}^* = B \mathbf{v}_2$  and the desired rotation matrix is defined as

$$R(\mathbf{n}_2, \theta) = I_{3 \times 3} \cos(\theta) + (1 - \cos(\theta)) \mathbf{n}_2 \mathbf{n}_2^T - \sin(\theta) [\mathbf{n}_2 \times] \quad (11)$$

Since the rotation is taking place about  $\mathbf{w}_1$ , then  $\mathbf{n}_2 = \mathbf{w}_1$  and by combining Eq. (7), Eq. (6) and Eq. (11), the following can be derived:

$$\begin{aligned} & \mathbf{w}_2^T \mathbf{w}_1 (\mathbf{w}_1^T B - \mathbf{v}_1^T) \mathbf{v}_2 - \|\mathbf{w}_1 \times \mathbf{w}_2\| \|\mathbf{v}_1 \times \mathbf{v}_2\| \\ &= \cos(\theta) (\mathbf{w}_2^T [\mathbf{w}_1 \times]^2 \mathbf{w}^*) \\ &+ \sin(\theta) (\mathbf{w}_2^T [\mathbf{w}_1 \times] \mathbf{w}^*) \end{aligned} \quad (12)$$

Note that the purpose of the initial rotation  $B$  was aligning the  $\mathbf{w}_1$  and  $\mathbf{v}_1$  vectors. This results in the first term on the left hand side of Eq. (12) to yield zero, and based on the observation geometry in Figure 2, the second term results in 1. Therefore, the equation can be simplified to the following form:

$$\begin{aligned} -1 &= \cos(\theta) \frac{\mathbf{w}_2^T [\mathbf{w}_1 \times]^2 \mathbf{w}^*}{\|\mathbf{w}_1 \times \mathbf{w}_2\| \|\mathbf{v}_1 \times \mathbf{v}_2\|} \\ &+ \sin(\theta) \frac{\mathbf{w}_2^T [\mathbf{w}_1 \times] \mathbf{w}^*}{\|\mathbf{w}_1 \times \mathbf{w}_2\| \|\mathbf{v}_1 \times \mathbf{v}_2\|} \end{aligned} \quad (13)$$

Using the identity  $\cos(\theta)\cos(\beta) + \sin(\theta)\sin(\beta)$  and replacing  $\cos(\beta)$  and  $\sin(\beta)$  with coefficients of  $\cos(\theta)$  and  $\sin(\theta)$  from Eq. (13), respectively, results in the final solution for the required rotation angle  $\theta$ :

$$\theta = \text{atan2}(\mathbf{w}_2^T[\mathbf{w}_1 \times] \mathbf{w}^*, \mathbf{w}_2^T[\mathbf{w}_1 \times]^2 \mathbf{w}^*) + \pi \quad (14)$$

It is clear by inspecting Eq. (13) that alignment of  $\mathbf{w}_1$  and  $\mathbf{w}_2$  and/or  $\mathbf{v}_1$  and  $\mathbf{v}_2$  vectors would result in an undefined solution as denominators in Eq. (13) would yield zero. In a physical sense, this is the case when both vehicles in formation and the common-observed object are positioned in a perfectly straight line with respect to each other [1].

## Final Solution

The final solution for the relative attitude of the vehicles in formation can be summarized using the equations:

$$B = \frac{(\mathbf{w}_1 + \mathbf{v}_1)(\mathbf{w}_1 + \mathbf{v}_1)^T}{1 + \mathbf{v}_1^T \mathbf{w}_1} - I_{3 \times 3} \quad (15a)$$

$$\mathbf{w}^* = B\mathbf{v} \quad (15b)$$

$$\theta = \text{atan2}(\mathbf{w}_2^T[\mathbf{w}_1 \times] \mathbf{w}^*, \mathbf{w}_2^T[\mathbf{w}_1 \times]^2 \mathbf{w}^*) + \pi \quad (15c)$$

$$R(\mathbf{w}_1, \theta) = I_{3 \times 3} \cos(\theta) + (1 - \cos(\theta))\mathbf{w}_1 \mathbf{w}_1^T - \sin(\theta)[\mathbf{w}_1 \times] \quad (15d)$$

$$A = R(\mathbf{w}_1, \theta)B \quad (15e)$$

These equations show that given one direction and one angle, a deterministic solution can be obtained for full three-axis relative attitude of two vehicles in formation [1].

## EXPERIMENTAL METHODS

To validate the accuracy and reliability of the three-axis relative attitude solution given by Ref. [1] and summarized in the previous sections, an experiment is set up at the University at Buffalo Controls and Automation Laboratory (CAL). CAL is equipped with the VICON Motion Capture System, which is capable of conducting passive optical motion capture. It has a series of infrared cameras positioned to capture and track movements of objects in the capture volume. The capture volume is simply a collection of all the points in a 3-dimensional space that can be observed and perceived by the VICON infrared cameras. The objects are observable using retroreflective markers which reflect the incoming infrared light beams

back to the cameras. The captured data is then transmitted to the VICON Tracker software installed on a PC and saved for processing. Once the optical cameras are calibrated with the VICON Active Wand to correct sensor edge distortion for synchronizing overlay across the observable volume, objects can be tracked by the system. Figure 3 demonstrates a general setup of the VICON Motion Capture System [10]. The experiment is the static formation of two quadcopters placed within a capture volume, similar to the one shown in Figure 3. Each quadcopter is equipped with five retroreflective markers to be recognized and observed by VICON as a distinct object. VICON system only requires three markers for full object detection, however the extra two markers can provide redundancy in case any of the markers becomes unobservable or falls outside of the capture volume. Four of the markers are placed on top of the rotor cases and the fifth marker is located on the approximate center of gravity of the quadcopter. Each object must be manually defined in the VICON software to become distinguishable. During this process, each vehicle acquires a unique body coordinate frame. Thus, VICON is capable of tracking both the position and the attitude of each object in the capture volume.

Before conducting the experiment, the camera calibration is performed using the VICON active wand. The wand is a T-shaped device with equidistant LED lights and the process consists of waving the wand against all cameras. The wand's trace can be observed real-time using the Tracker software and the objective is to cover as much of the capture volume as possible to avoid view field edge distortions and achieve proper camera synchronization. Once the calibration is complete, the two quadcopters equipped with the aforementioned retroreflective markers are placed in the capture volume with random attitudes. The VICON Tracker software is used to define and distinguish each quadcopter by giving them a name and a body reference frame. The quadcopters are defined as *Drone 1* and *Drone 2* in the Tracker software. Once the setup is complete, the Tracker software is commanded to start the recording process and the data consists of the full inertial attitude of *Drone 1* and *Drone 2*, denoted  $A_I^{B_1}$  and  $A_I^{B_2}$ , respectively, as well as the individual position information of each marker, of which there ten in total. This information is recorded for approximately thirty minutes, resulting in 50,000 data points. The origin of the inertial reference frame of VICON capture volume is treated as a common-observed object <sup>1</sup> and all position and attitude information for both vehicles are saved for post processing.

<sup>1</sup>In this experiment the location of the common observed object is used to determine  $\mathbf{v}_2$  and  $\mathbf{w}_2$  vectors. However, with the implementation of laser communication devices these measurements can be acquired without the position information of the common object. Therefore, the previous conclusion on the position of the common object not being necessary is not being violated.

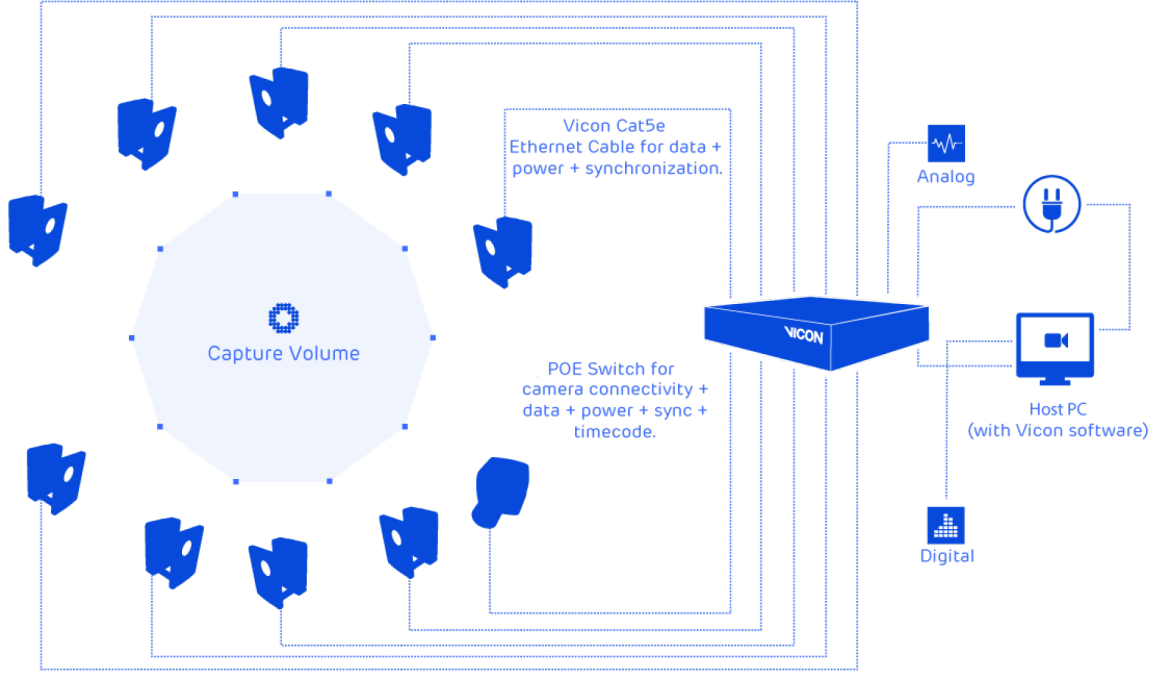


Figure 3: VICON Physical Setup

## EXPERIMENTAL RESULTS

The required LOS vectors are computed by employing the appropriate transformations on the position vectors captured by VICON and shown below using the measurement and estimate notation:

$$\tilde{\mathbf{v}}_1 = A_{\mathcal{I}}^{\mathcal{B}_1}(\mathbf{r}_1 - \mathbf{r}_2) \quad (16a)$$

$$\tilde{\mathbf{v}}_2 = A_{\mathcal{I}}^{\mathcal{B}_1} \mathbf{r}_1^{\mathcal{I}} \quad (16b)$$

$$\tilde{\mathbf{w}}_1 = A_{\mathcal{I}}^{\mathcal{B}_1}(\mathbf{r}_1 - \mathbf{r}_2) \quad (16c)$$

$$\tilde{\mathbf{w}}_2 = A_{\mathcal{I}}^{\mathcal{B}_2} \mathbf{r}_2^{\mathcal{I}} \quad (16d)$$

where  $\mathbf{r}_i$  are the unit position vectors of vehicles  $i$  (defined as the marker on the COG) described in inertial coordinate frame  $\mathcal{I}$ . Due to the high signal-to-noise ratio (SNR) of the VICON system, a simple median filter is applied to filter any possible noise in the position and attitude data. An example of the filter in action is shown in Figure 4.

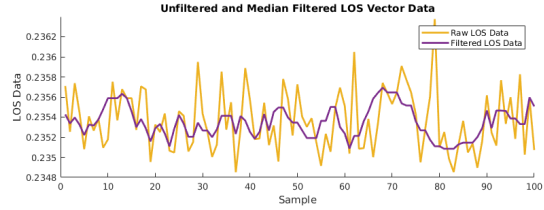


Figure 4: Demonstration of median filter on LOS vector data

The attitude of each vehicle is recorded by the VICON Tracker software as a  $1 \times 9$  array such that it constructs a row by row concatenation of the attitude matrix. First, each of these  $1 \times 9$  arrays is converted to a proper  $3 \times 3$  attitude matrix and then the relative attitude providing the mapping between  $\mathcal{B}_1$  and  $\mathcal{B}_2$  frames is determined by the following:

$$A_{\mathcal{B}_1}^{\mathcal{B}_2} = A_{\mathcal{I}}^{\mathcal{B}_1} A_{\mathcal{I}}^{\mathcal{B}_2^T} \quad (17)$$

where  $A_{\mathcal{B}_1}^{\mathcal{B}_2}$  is treated as the estimated attitude, determined by VICON, denoted as  $\hat{A}$ , here on and shown below:

$$\hat{A} = \begin{bmatrix} 0.9158 & -0.3998 & -0.0331 \\ 0.3978 & 0.9159 & -0.0535 \\ 0.0517 & 0.0358 & 0.9979 \end{bmatrix}$$

To compare the results of the experiment and the pro-

posed solution, the true attitude matrix is determined using Eq. (15). The LOS vectors computed using the VI-CON position information are used as inputs to these equations, after the median filter implementation. The resulting true attitude matrix is

$$A_{\text{true}} = \begin{bmatrix} 0.9163 & -0.3992 & -0.0282 \\ 0.3975 & 0.9159 & -0.0538 \\ 0.0473 & 0.0381 & 0.9981 \end{bmatrix}$$

It is clear that the estimated and the true attitude matrices lie very close to one another. A discussion on the covariances of estimated and true attitude matrices is provided in the following sections to further investigate the accuracy of the proposed solution in comparison to the experimental results.

## ATTITUDE-ERROR COVARIANCE MATRIX

To evaluate the accuracy of the proposed solution, the attitude-error covariance matrix (ECM) is used, which represents the local second-order moment of the probability density function of the error in the estimate. Reference [1] discusses in detail, computing the ECM by assuming the planar constraint. Consider the following estimate representations of the LOS vectors with noise:

$$\tilde{\mathbf{w}}_1 = \mathbf{w}_1 + v_{w_1}, v_{w_1} \sim \mathcal{N}(\mathbf{0}, R_{w_1}) \quad (18a)$$

$$\tilde{\mathbf{w}}_2 = \mathbf{w}_2 + v_{w_2}, v_{w_2} \sim \mathcal{N}(\mathbf{0}, R_{w_2}) \quad (18b)$$

$$\tilde{\mathbf{v}}_1 = \mathbf{v}_1 + v_{v_1}, v_{v_1} \sim \mathcal{N}(\mathbf{0}, R_{v_1}) \quad (18c)$$

$$\tilde{\mathbf{v}}_2 = \mathbf{v}_2 + v_{v_2}, v_{v_2} \sim \mathcal{N}(\mathbf{0}, R_{v_2}) \quad (18d)$$

where  $v$  represents the noise in each measurement. Previously, the triangular constraint was introduced to obtain an unambiguous solution for the relative attitude. In this section the planar constraint will be used to compute the ECM. Furthermore, the consistency and compatibility of the ECM with triangle constraint will be discussed.

### Planar Constraint ECM

In the planar constraint case, Eq. (1) must still be satisfied, which can be written in measurement and estimate notation as

$$\tilde{\mathbf{w}}_1 = \hat{A} \tilde{\mathbf{v}}_1 \quad (19)$$

However, instead of satisfying Eq. (7), which is the triangle constraint equation, Eq. (2) must be enforced to ensure all observations lie on the same plane. This can also be

written in the measurement and estimate notation as the following:

$$0 = \tilde{\mathbf{w}}_2^T [\tilde{\mathbf{w}}_1 \times] \hat{A} \tilde{\mathbf{v}}_2 \quad (20)$$

The present ambiguity of the planar constraint solution is not problematic when computing the error covariance; the final ECM derived will satisfy both solutions, which are  $\theta$  and  $\theta + \pi$  rotations, hence the twofold ambiguity does not need to be resolved for the purposes of computing the desired ECM. The preceding two equations can be rewritten in vector form

$$[\tilde{\mathbf{w}}_1^T \quad 0]^T = [(A_{\text{true}} \mathbf{v}_1)^T \quad \mathbf{w}_2^T [\mathbf{w}_1 \times] A_{\text{true}} \mathbf{v}_2]^T + \Delta \quad (21)$$

where  $\Delta = [\Delta_1^T \quad \Delta_2^T]^T$  is the error in the measurements. The first term on the right hand side of Eq. (21) is the true output, which is a function of  $A_{\text{true}}$ . By naming the true output as  $\mathbf{h}(A_{\text{true}})$  and the measurement vector as  $\tilde{\mathbf{y}}$ , Eq. (21) can be simplified as

$$\tilde{\mathbf{y}} = \mathbf{h}(A_{\text{true}}) + \Delta \quad (22)$$

The following expression is defined as the covariance of the measurement error vector  $\Delta$  [1]:

$$\mathcal{R} = \begin{bmatrix} R_{\Delta_1} & R_{\Delta_1 \Delta_2} \\ R_{\Delta_1 \Delta_2}^T & R_{\Delta_2} \end{bmatrix} \quad (23)$$

To compute the elements of  $\mathcal{R}$ , the covariance of each LOS measurement must be known. This can simply be computed using the “cov” command in Matlab and the LOS measurement covariances can be expressed as the following:

$$R_{v_1} = \text{cov}(\tilde{\mathbf{v}}_1) \quad (24a)$$

$$R_{v_2} = \text{cov}(\tilde{\mathbf{v}}_2) \quad (24b)$$

$$R_{w_1} = \text{cov}(\tilde{\mathbf{w}}_1) \quad (24c)$$

$$R_{w_2} = \text{cov}(\tilde{\mathbf{w}}_2) \quad (24d)$$

Now the following expressions can be defined as the individual elements of the covariance matrix  $\mathcal{R}$ :

$$R_{\Delta_1} = R_{w_1} + A_{\text{true}} R_{v_1} A_{\text{true}}^T \quad (25)$$

$$\begin{aligned} R_{\Delta_1} = & - \{ \mathbf{w}_2^T [A_{\text{true}} \mathbf{v}_2 \times] R_{w_1} [A_{\text{true}} \mathbf{v}_2 \times] \mathbf{w}_2 \\ & + (A_{\text{true}} \mathbf{v}_2)^T [\mathbf{w}_1 \times] R_{w_2} [\mathbf{w}_1 \times] (A_{\text{true}} \mathbf{v}_2) \\ & + \mathbf{w}_2^T [\mathbf{w}_1 \times] A_{\text{true}} R_{v_2} A_{\text{true}}^T [\mathbf{w}_1 \times] \mathbf{w}_2 \} \end{aligned} \quad (26)$$

$$\begin{aligned} R_{\Delta_1 \Delta_2} = & E \{ (v_{w_1} - A_{\text{true}} v_{v_1}) (\mathbf{w}_2^T [A_{\text{true}} \mathbf{v}_2 \times] v_{w_1} \\ & - \mathbf{w}_2^T [\mathbf{w}_1 \times] A_{\text{true}} v_{v_2} + (A_{\text{true}} \mathbf{v}_2)^T [\mathbf{w}_1 \times] v_{w_2}) \} \end{aligned} \quad (27)$$

Now that the covariance matrix of the measurement vector,  $\mathcal{R}$ , is known, the attitude ECM can be computed using the following expression:

$$P_{\delta_\alpha \delta_\alpha} = (\mathcal{H}^T \mathcal{R}^{-1} \mathcal{H})^{-1} \quad (28)$$

where

$$\mathcal{H} = \begin{bmatrix} -[A_{\text{true}} \mathbf{v}_1 \times] \\ -\mathbf{w}_2^T [\mathbf{w}_1 \times] [A_{\text{true}} \mathbf{v}_2 \times] \end{bmatrix} \quad (29)$$

### Triangle Constraint ECM

By inspecting Eq. (28), it is clear that the  $\mathcal{H}$  matrix must have linearly independent rows and columns, in other words have a full rank, for  $P_{\delta_\alpha \delta_\alpha}$  to exist. However, it is demonstrated in Ref. [1] the redefined  $\mathcal{H}$  for the triangle constraint does not meet this requirement. Therefore, the desired attitude ECM can only be derived by assuming the planar constraint. However, the triangle constraint does not enforce the LOS vectors to be constrained in the same plane and therefore any out-of-plane deflection will result in attitude errors. To resolve the aforementioned issue, the covariance of the estimate attitude is computed in the next section and it is demonstrated that the attitude covariance computed using Eq. (28) bounds the yaw, pitch and roll angle errors.

## ESTIMATE ATTITUDE COVARIANCE

The ECM in the estimate attitude,  $\hat{A}$ , is computed to be compared with the true attitude ECM. First,  $\hat{A}$  is converted to the quaternion form by employing the following set of equations [5]:

$$q_4 = \pm \frac{1}{2} \sqrt{1 + \text{trace}(\hat{A})} \quad (30a)$$

$$q_1 = \frac{1}{4q_4} (\hat{a}_{23} - \hat{a}_{32}) \quad (30b)$$

$$q_2 = \frac{1}{4q_4} (\hat{a}_{31} - \hat{a}_{13}) \quad (30c)$$

$$q_3 = \frac{1}{4q_4} (\hat{a}_{12} - \hat{a}_{21}) \quad (30d)$$

$$\hat{\mathbf{q}} = \begin{bmatrix} \mathbf{q}_{1:3} \\ q_4 \end{bmatrix} \quad (31)$$

Having acquired the quaternion representation of the estimate attitude using the above equations, a quaternion averaging technique can be adopted to eventually compute the small roll, pitch and yaw angle errors [3].

### Averaging Quaternions

An important step in calculating the error covariance matrix is in finding the average of the measured quaternion

data. The mathematical basis of the process is described in Ref. [3]. Given a set of weights  $w_i$  for the quaternions (where in the case of this paper, all weights are set to 1) a matrix  $M$  is defined as:

$$M \triangleq \sum_{i=1}^n w_i \mathbf{q}_i \mathbf{q}_i^T \quad (32)$$

where  $\mathbf{q}_i$  are the quaternion vectors to be averaged. Then, the average of the quaternions is found by the maximization procedure:

$$\bar{\mathbf{q}} = \text{argmax } \mathbf{q}^T M \mathbf{q} \quad (33)$$

The solution to the procedure is then just the eigenvector of  $M$  corresponding to the maximum eigenvalue [3].

Using this method, the average estimated quaternion is determined to be

$$\bar{\mathbf{q}} = \begin{bmatrix} 0.0228 \\ -0.0217 \\ 0.2038 \\ -0.9785 \end{bmatrix} \quad (34)$$

The quantity  $\hat{\mathbf{q}}$  can now be used to determine the error quaternion,  $\delta \mathbf{q}$ , which is related to the small angle errors by

$$\delta \mathbf{q} \approx \begin{bmatrix} \frac{1}{2} \delta \boldsymbol{\alpha} \\ 1 \end{bmatrix} \quad (35)$$

where  $\delta \mathbf{q}$  is computed by crossing the average quaternion with the inverse of the estimate attitude quaternion [1]:

$$\delta \mathbf{q} = \bar{\mathbf{q}} \otimes \hat{\mathbf{q}}^{-1} \quad (36)$$

Since the VICON system outputs the position and attitude information of *Drone 1* and *Drone 2* at every time stamp, consequently,  $\delta \boldsymbol{\alpha}$  is a  $3 \times 50000$  matrix where each row represents the roll, pitch and yaw angle errors, respectively, while each column corresponds to a particular time stamp. Therefore, the covariance of such matrix would return a  $3 \times 3$  matrix, which is defined as the estimate attitude ECM:

$$\mathcal{R}_{\text{Est}} = \text{cov}(\delta \boldsymbol{\alpha}) \quad (37)$$

The results of the comparison are demonstrated in the FINAL RESULTS section of this paper.

## DIVERGENCE

When considering the methods by which the true and estimated relative attitude information are extracted, concerns may arrive regarding the source of information and data being common for the estimated relative attitude and the LOS information used to extract the true relative attitude.

To address and resolve such concerns on double-counting, the following is introduced.

An alternative method for comparing the estimated and true relative attitude results is examining the distance between the covariance matrix of the estimated attitude and the true attitude at multiple timesteps. This is achieved by calculating a covariance distance metric, of which there are many, such as the Bhattacharya distance or the Jensen-Shannon divergence. Here, a measure introduced by Herdin et al. is chosen, as it overcomes any issues associated with double counting by not assuming correlation [4]. The equation is given by

$$d = 1 - \frac{\text{trace}(R_1 \cdot R_2)}{\|R_1\| \cdot \|R_2\|} \quad (38)$$

where  $d$  is the distance, and  $R_1$  and  $R_2$  are the covariance matrices being compared. The distances between the covariance matrix generated for the estimated attitude and the covariance matrix generated for the true attitude at random sample points are shown in Figure 5. The measure is bounded between 0 and 1; it returns 0 if the two matrices are equal and 1 if there is no similarity at all.

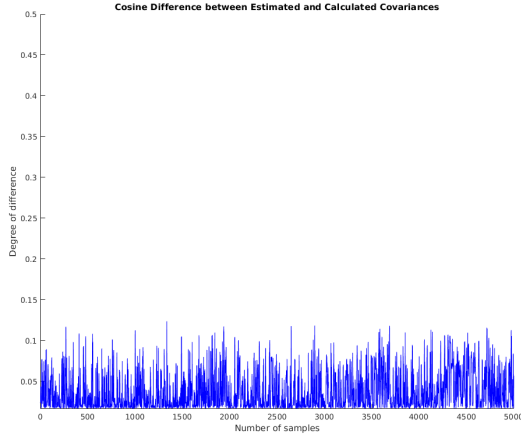


**Figure 5: Truth and Estimate ECM Correlation**

The graph shows the degree of variance in the metric, which has mean  $\mu = 0.0365$ , which indicates a high degree of accuracy in the algorithm.

## FINAL RESULTS

Previously, in the Averaging Quaternions section, it was shown that the true attitude  $A_{\text{true}}$ , determined by the proposed solution, and the estimated attitude  $\hat{A}$ , given by the

VICON system are highly compatible. Further investigation on the attitude error covariance matrix provided similar grounds to show good performance characteristics. Analytical results showed that the attitude covariance bounds the small roll, pitch and yaw angle errors determined previously, in a  $3\sigma$  sense, as shown in Figure 6.

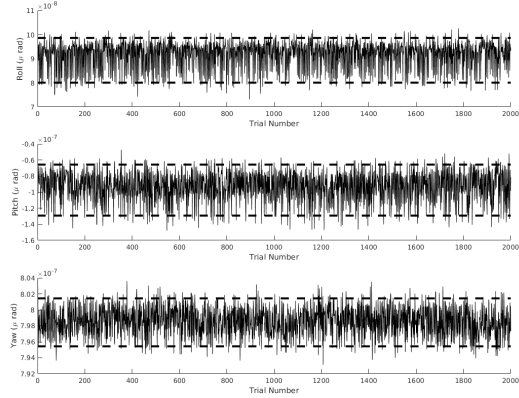


**Figure 6: Relative Attitude Estimate Errors**

$$P_{\delta\alpha\delta\alpha} = 1 \times 10^{-3} \begin{bmatrix} 0.0636 & -0.1448 & 0.0010 \\ -0.1448 & 0.4564 & -0.0143 \\ 0.0010 & -0.0143 & 0.0028 \end{bmatrix}$$

The dashed lines in Figure 6 are the  $3\sigma$  bounds. The curves bounded in between these bounds correspond to the roll, pitch, and yaw angle errors in each subplot, respectively. The results are consistent with the hypothesis and simulations demonstrated in Ref. [1], and adequately show the accuracy of the proposed algorithm for GPS-denied relative attitude determination for static formation of any two vehicles with a set of LOS observations.

## CONCLUSIONS

This paper presented a verification of a new approach to determine the relative attitude between two vehicles. The approach is self-contained in that no external sensors, such as GPS, are required to determine the relative attitude. Line-of-sights between the vehicles and to a common object are only required to obtain a solution. The novel aspect of the approach is that no information on the common object is required, i.e. its position is not required to be known. It is only required that both vehicles know that the object is common to a both. Hence, a catalog of objects is not required, which is a clear advantage over existing GPS-denied approaches that require objects be both



associated and identified from a catalog. The experiments show that the approach is a viable one, and provide a basis for optimism that it can be translated into a real working system.

## REFERENCES

- [1] Linares, R., Crassidis, J.L., and Cheng, Y., “Constrained Relative Attitude Determination for Two-Vehicle Formations,” *Journal of Guidance, Control, and Dynamics*, Vol. 34, No. 2, March-April 2011, pp. 543-553. doi:10.2514/1.50053.
- [2] Markley, F.L., and Crassidis, J.L., *Fundamentals of Spacecraft Attitude Determination and Control*, Springer, New York, NY, 2014.
- [3] Markley, F.L., Cheng, Y., Crassidis, J.L., and Oshman, Y., “Averaging Quaternions,” *Journal of Guidance, Control, and Dynamics*, Vol. 30, No. 4, July-Aug. 2007, pp. 1193-1196. doi:10.2514/1.28949.
- [4] Herdin, M., Czink, N., Ozelik, H., and Bonek, E., “Correlation Matrix Distance, a Meaningful Measure for Evaluation of Non-Stationary MIMO Channels,” *IEEE 61st Vehicular Technology Conference*, Stockholm, Sweden, May-June 2005, doi:10.1109/VETECS.2005.1543265.
- [5] Schaub, H., and Junkins, J.L., *Analytical Mechanics of Space Systems*, 2<sup>nd</sup> Edition, American Institute of Aeronautics and Astronautics, Reston, VA, 2014.
- [6] Crassidis, J.L., Junkins, J.L., *Optimal Estimation of Dynamic Systems*, 2<sup>nd</sup> Edition, CRC Press, Boca Raton, FL, 2012.
- [7] Gopalarathnam, A., “Aerodynamic Benefit of Aircraft Formation Flight,” *Encyclopedia of Aerospace Engineering*, Dec. 2010. doi:10.1002/9780470686652.eae023.
- [8] Bangash, Z., Ahmed, A., Khan, J., and Sanchez, R.P., “Aerodynamics of Formation Flight,” *Journal of Aircraft*, Vol. 43, No. 4, July 2006, pp. 907-912. doi:10.2514/1.13872.
- [9] Olsen, N., Friis-Christensen, E., and Floberghagen, R., “The Swarm Satellite Constellation Application and Research Facility (SCARF) and Swarm Data Products,” *Earth Planet Space*, Vol. 65, 2013, pp. 1189-1200. doi:10.5047/eps.2013.07.001.
- [10] VICON. *What is Motion Capture*. Retrieved from <https://www.vicon.com/what-is-motion-capture>.